

# Clustered Mobility Model for Scale-Free Wireless Networks

Sunho Lim      Chansu Yu<sup>†</sup>      Chita R. Das<sup>‡</sup>  
Dept. of EECS      †Dept. of ECE      ‡Dept. of CSE  
South Dakota State University      Cleveland State University      The Pennsylvania State University  
Brookings, SD 57007      Cleveland, OH 44115      University Park, PA 16802  
sunho.lim@sdstate.edu      c.yu91@csuohio.edu      das@cse.psu.edu

**Abstract**—Recently, researchers have discovered that many of social, natural and biological networks are characterized by scale-free power-law connectivity distribution and a few densely populated nodes, known as hubs. We envision that wireless communication or sensor networks are directly deployed over such real-world networks to facilitate communication among participating entities. Here nodes move in such a way that they exhibit scale-free connectivity distribution at any instance, which cannot be modeled by most of the prior mobility models such as random waypoint (RWP) mobility model. This paper proposes clustered mobility model (CMM), which facilitates in forming hubs in a network satisfying the scale-free property. We call this a scale-free wireless network (SFWN). In CMM, it is possible to control the degree of node concentration or non-homogeneity to easily assess the strengths and weaknesses of the scale-free phenomena. To the best of the authors’ knowledge, there has been no such mobility model reported in the literature and we believe the proposed CMM can be usefully used to investigate the properties of the SFWNs that are likely to occur in a real deployment of wireless multihop and sensor networks. Another important feature of CMM is that it does not possess any unintended spatial and temporal characteristics found in other mobility models such as RWP. Finally, to highlight the difference between a SFWN and a conventional wireless network, extensive simulation study has been conducted to measure network capacities at the physical, link and network layers.

**Index Terms**—Connectivity distribution, mobility model, network capacity, random waypoint mobility, scale-free wireless networks.

## I. INTRODUCTION

Recently there has been considerable interest in the structure and dynamics of large complex networks found in natural, technological and social networks [1], [2]. Random graphs [3] are often used to model such complex networks. However, real-life networks<sup>1</sup> have consistently shown that their topologies deviate from uncorrelated random graphs in many respects [4]. New graph models, known as *small-world graph* [1] and *scale-free networks* [2], have been suggested to capture the correlation. The former is characterized by high degree of clustering. A unique characteristic of the latter is scale-free power-law connectivity distribution, *i.e.*, the probability  $p_k$  that a vertex has  $k$  connectivity is proportional to  $k^{-\beta}$ , where  $\beta$  tends to fall between 2 and 3. It explains the existence of hubs

whose connectivities are much larger than that of an average node [2].

Scale-free networks have been observed in many real-world scenarios and a communication network is often desired over such scenarios to facilitate communication among participating entities. In such a network, nodes do not move randomly but follow the scale-free pattern. In other words, at any instance, connectivity distribution of nodes is scale-free, thus we call it a *Scale-Free Wireless Network (SFWN)*. This motivated us to consider how to model such node mobility and how it affects the network behavior. The adverse impact of hub nodes on network performance has been addressed recently [5], [6]. Kawadia and Kumar [5] noted the performance degradation due to non-homogeneous distribution of nodes and proposed CLUSTERPOW and MINPOW algorithms to mitigate the problem. Wang and Li [6] pointed out the possibility of node concentration and focused on the corresponding network partition problem. In [7], network performance degrades also observed due to hubs because nodes in their vicinity experience excessive contention, congestion and resource depletion and thus they become the bottlenecks in the network. However, none of these research pays attention to how hub nodes are created, how to model them and what is the fundamental impact on network performance.

This paper proposes a novel mobility model, called *Clustered Mobility Model (CMM)*, where nodes tend to move closer to highly connected nodes, resulting in node clustering around hubs and thus a SFWN. This is a clear contrast to conventional random mobility models such as *Random Waypoint (RWP)* [8], in which nodes are assumed to move randomly and thus their locations are scattered almost uniformly across the entire network area. To the best of the authors’ knowledge, there has been no such study reported in the literature. It is important to note that the CMM is designed to possess consistent steady-state mobility parameters. This is crucial in a simulation-based study of mobile networks for correct evaluation of a system or a protocol [9]. It has been discovered that conventional mobility models such as RWP exhibit unintended spatial and temporal characteristics. For example, node speed does not reach steady state [10], [11], [12], [13], [9] and nodes tends to be cluttered at the center of the network as simulation time progresses [14], [15], [16], [9], [17], [11]. In CMM, a special care has been taken so that nodes do not show any biased, unintended movement during the entire period of simulation

This research was supported in part by Startup grant of Dept. of EECS in SDSU.

<sup>1</sup>They include electric power grid, the World Wide Web, the Internet backbone, collaboration and citation networks in the scientific community, and US airline connection networks.

time.

Using CMM, this paper reveals the performance implication of non-homogeneous node distribution in a SFWN in terms of network capacity. While network capacity is a fundamental measure of a wireless network, previous studies have evaluated at one particular level, which may not accurately assess the true performance of a network or a system. This paper defines it at all relevant layers in their abstract form (see Section IV.A for definitions on PHY, MAC, and NET capacities) and investigate differences between a SFWN and a conventional wireless network in terms of the three capacities.

This paper is organized as follows. Section II discusses related work on scale-free networks in general and mobility models developed for wireless ad hoc networks. Section III presents the proposed CMM that results in a SFWN. Section IV is devoted to the performance analysis of SFWNs and conventional wireless networks in terms of network capacities. Section V concludes our work.

## II. BACKGROUND AND RELATED WORK

This section discusses several ingredients in developing CMM and characterizing SFWNs. First of all, Section II.A introduces recent studies on small-world and scale-free networks in general sense. It also discusses recent study on *spatial scale-free networks* in which two nodes are considered connected when the Euclidean distance between the two is smaller than a cutoff distance. This is particularly interesting because it directly translates to packet radio networks with finite transmission range. Section II.B overviews previous research on mobility as our focus in this paper is to develop a mobility model that results in scale-free connectivity distribution. In particular, it discusses why steady-state mobility parameters are important in simulation-based research, and how non-homogeneous node distribution arises and how it is modeled.

### A. Scale-Free Networks

Scientists have recently discovered that various complex networks such as Internet and social networks exhibit interesting topological properties not found in simple random networks. Watts and Strogatz [18] introduced *small-world graphs*, which exhibits small world property as well as high degrees of clustering. Barabasi and Albert [19] have studied the World Wide Web and found that connectivity distribution follows a power law<sup>2</sup>. It renders highly connected nodes or hubs to have a large chance of occurring, which is unusual in random networks. They call networks containing hubs *scale-free* in the sense that some hubs have a seemingly unlimited connectivity and no node is typical of the others<sup>3</sup> [19].

A scale-free network has been explained with two generic mechanisms: *incremental growth* and *preferential attachment* [2]. As new nodes appear, they tend to connect to the more connected nodes. In other words, the probability  $\varphi_i$  that a

new node will be connected to a node  $i$  depends on the connectivity  $k_i$  of that node, *i.e.*,  $\varphi_i = \frac{k_i+1}{\sum_j (k_j+1)}$  [2]. It was shown analytically that these mechanisms lead to the power-law connectivity distribution, *i.e.*,  $p_{k_i} \propto k_i^{-\beta}$ , where  $p_{k_i}$  denotes the probability that a node has  $k_i$  connectivity [23]. For reasons not yet known, the value of  $\beta$  tends to fall between 2 and 3 [2].

An extended model has been introduced in [23], [24] to give a more realistic description of the local processes such as *rewiring*. It allows for some additional flexibility in the formation of networks by removing links connected to certain nodes and replacing them by new links in a way that effectively amounts to a local type of re-shuffling connections [24].

It is important to note that majority of small-world and scale-free networks assume *relational graph model* where distance is measured only by graph itself. Wireless ad hoc networks as well as some real-life networks such as routers of the Internet and transportation networks are embedded in physical Euclidean space and possess a geography in addition to their topology. The spatial location of nodes and their geographical proximity completely determines the connectivity among the nodes [25], [26], [4]. In this type of *spatial graphs*, two neighbors of a node have a better chance to be a neighbor with each other, which is not necessarily true in relational graphs. Large connectivities are usually obtained in high density regions, called *hub areas*, and therefore, small-world graphs exhibit scale-free property or vice versa unlike in relational graphs [26].

### B. Steady-State Mobility Parameters

This subsection discusses several mobility models proposed in the literature and summarizes earlier work concerning steady-state parameters and node concentration in those mobility models.

1) *Mobility Models*: Mobility models can be divided into *individual* and *group mobility models*, where the difference lies whether or not the position and movement pattern of a mobile host is independent of other nodes [27]. Random Walk or Brownian Motion is an individual mobility model that emulates the erratic movement of various entities in nature and also in wireless mobile networks [28]. Disadvantage of this model is that it results in sharp turns and sudden stops. RWP has been proposed in [8] and overcomes the shortcomings of Random Walk model. Mobility models such as *Manhattan Mobility Model* and *Obstacle Mobility Model* [27] are a step forward towards realistic mobility model but their applicability is limited to some particular applications and the selection of node destination and initial distribution is based on RWP.

Another interesting area of adding practicality in mobility models is group mobility [6], [29], [30], wherein a group of nodes share a common mobility pattern. Hong *et al.* proposed *Random Point Group Mobility model (RPGM)* [6]. According to this model, each group has a logical center and the movement pattern of a logical center controls that of its member nodes including speed, direction, and acceleration, etc.

<sup>2</sup>Heavy-tail power law distributions have recently been observed from many measurement studies of computer and communication systems, where the exponential distribution has been traditionally assumed, *i.e.*, network traffic [20], I/O traffic, Unix process lifetime [21], and file sizes in the Web [22].

<sup>3</sup>Extremes on the other side are completely ordered (*e.g.*, mesh) or completely random networks. Statistical property in a local structure mirrors its global structure [18].

2) *Temporal mobility parameter - Node speed*: Recently, researchers in the area of mobility model concentrate not only on developing realistic ones but also answering whether they provide consistent steady-state mobility parameters during simulation. Consider the RWP, for instance, where nodes repeat the pause-and-mobility cycles. Since the node speed is chosen uniformly from  $[0, V_{max}]$ , we expect that the average node speed is  $\frac{V_{max}}{2}$  at steady state. However, it has been discovered that the RWP fails to provide a steady state node speed during simulation [10], [11], [12], [13]. In other words, average node speed reaches zero as simulation progresses because when a node selects a very low speed in  $[0, V_{max}]$  it would continue to use the same speed without reaching the specified waypoint until the simulation ends. In the long run, more number of nodes get stuck with such situation and thus, the average node speed diminishes. A simple, although not perfect, solution is to use non-zero minimum speed [9], which is adopted in CMM as explained in Section III.

3) *Spatial mobility parameter - Node positions*: More relevant to our research, it has been shown that RWP does not exhibit truly random spatial, topological properties [14], [15], [16], [9]. Royer *et al.* showed that average node connectivity changes over time in RWP and nodes are more concentrated at the center of simulation area as time progresses [17]. This motivated them to propose *Random Direction mobility model (RWP\_D)*, where a mobile node selects a random direction and speed and starts moving until it reaches the simulation boundary along that direction. Once the boundary is reached, the mobile node pauses for a specified time, then chooses another direction between  $(0, \pi)$  and the process continues.

However, many nodes following RWP\_D are located at boundaries [11] while nodes following RWP tend to be cluttered at the center of the network, either of which is not intended and not desirable. We propose a simple modification that leads to a satisfactory node distribution even though it may not be realistic: *Random waypoint with wrap-around mobility model (RWP\_WRAP)*. It follows the same movement as in RWP except that the network is wrap-around. RWP\_WRAP has been adopted in CMM and used as a reference mobility model for comparison purpose in Section IV.

4) *Spatial mobility parameter - Node density*: One important observation in most of the mobility models discussed in the literature is that they all produce random locations of nodes so that nodes are well balanced and scattered across the entire network area (except the unintended centering or boundary effect mentioned above).

Consider the spatial distribution of nodes in a network area with RWP. Assume that the entire area is divided into a number of equal-sized subareas. Each node is positioned in a particular subarea with independent probability,  $\varphi$ , which is the reciprocal of the number of subareas,  $s_t$ . The probability  $p_k$  that a subarea has exactly  $k$  nodes is given by the *binomial distribution*,  $p_k = C_k^n \varphi^k (1 - \varphi)^{n-k}$ , where  $n$  is the total number of nodes. As a limiting case, this probability becomes the well-known *Poisson distribution*  $p_k = \frac{z^k e^{-z}}{k!}$ , where  $z$  is the mean number of nodes in a subarea, which is equal to  $n\varphi$  or  $\frac{n}{s_t}$ . Both binomial and Poisson distributions are strongly peaked about the mean  $z$ , and have a heavy- $k$  tail

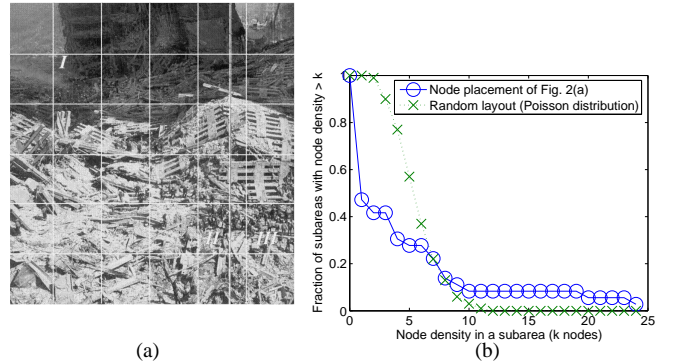


Fig. 1. Node distribution in an example ad hoc network. (a) Rescue team at Ground Zero [31]. (b) Node density distribution

that decays rapidly as a function of  $\frac{1}{k!}$  [18]. In other words, with the random node locations, the majority of subareas have similar number of nodes and significant deviations from the average case (e.g., a subarea with a large fraction of nodes) is extremely rare.

In a real network of mobile nodes, however, the node distribution can be very different from the Poisson distribution. For example, Figure 1(a) shows an example of a disaster area where the infrastructure-less ad hoc network is well suited for supporting communication. Many rescue team members gather at three hub subareas, denoted as I, II and III in the figure, which may be a base camp or have many casualties. The three subareas out of 36 ( $s_t = 36$ ) include about the half of the total rescue team members (66 out of 137). Figure 1(b) shows the node density distribution of the disaster area in Figure 1(a) as well as that of the random node locations that follows the Poisson distribution. It is clear from Figure 1(b) that RWP does not model the node distribution of a real ad hoc network situation. Even in the presence of node mobility, node concentration would persist because, for example in Figure 1(a), a mobile node (*i.e.*, a rescue team member) leaving a hub subarea is most likely to move to another hub subarea. As evident in Figure 1(b), the corresponding node distribution contains a heavy-tail unlike the Poisson distribution. It can be modeled by a power law distribution, which has been discussed in Section II-A. And, the main cause of this phenomenon can be explained using the principle of preferential attachment also described in the same section.

The main question in this paper is therefore how to model such a non-uniform node distribution. [32] explains methods to generate node clustering and results in a clustered distribution of nodes, but it just generates node concentration for initial node locations and does not include mobility.

### III. CLUSTERED MOBILITY MODEL

This section presents a new mobility model for clustered scenarios termed as the *Clustered Mobility Model (CMM)*. We call a wireless multihop network a *Scale-Free Wireless Network (SFWN)* when nodes follow CMM as their mobility pattern.

#### A. Synthesis of CMM

The model can be visualized to consist of two steps, the first being to generate the initial layout and the second being

the selection of waypoints to induce mobility. Pause times and node speed are selected as in RWP\_WRAP. The difference lies in selecting the initial layout and waypoints. The two steps correspond to *growth* [2] and *rewiring* [23] [24] (see Section II-A), both of which are based on the principle of preferential attachment [2]. However, CMM applies it differently: The entire simulation area is logically divided into a number of subareas. Then, a node is attracted more to a highly populated subarea than to a sparse subarea. In other words, during both the growth and rewiring step, a node  $n_x$  is attracted to a subarea  $s_i$  with a higher probability than  $s_j$  if  $s_i$  has more number of nodes than  $s_j$ .

The first step of CMM (growth) is to generate an initial layout. Initially all subareas have no nodes, and therefore, the probability of a subarea being assigned the next node is equal. But as a new node is assigned to a different subarea, its probability increases or decreases depending on the present number of nodes. For example, if a subarea  $s_i$  has  $k_i$  nodes, its probability,  $\varphi_i$ , is  $\frac{(k_i+1)^\alpha}{\sum_j (k_j+1)^\alpha}$ , where  $\alpha$  is the clustering exponent. During the process, some subareas will have a higher probability than others and will become the hub areas. Nodes are randomly located within the chosen subareas. The growth process ends when all the pre-determined number of nodes have been assigned subareas. The initial layout is the outcome of this process. Final  $\varphi_i$ 's will be used in the next step and won't be changed during the simulation.

The second step of CMM (rewiring) is to induce mobility. Each node is rewired from one subarea to another when it repeats the pause-and-mobility cycles. A waypoint is selected by, first of all, choosing a subarea and then choosing a position within that subarea. The choice of a subarea is based on the principle of preferential attachment using  $\varphi_i$ 's. The node selects a speed, which is uniformly distributed between  $[V_{min}, V_{max}]$  and starts moving towards it. Here,  $V_{min}$  is set to nonzero to achieve a steady-state node speed as discussed in the previous section.

It is important to note that the level of node concentration in the initial layout would be greatly reduced during the mobility step. This is because nodes are not only rewired to waypoints but also travel in between the waypoints. While waypoints are chosen based on the preferential attachment mechanism, node position between the waypoints is considered random. A node is randomly located in the network for some percentage of its lifetime and located in a scale-free fashion for the rest of the time. We call this percentage as *mobility fraction*,  $\xi$ , which will play a key role to derive steady-state subarea population.

However, how long does it take for the network to reach a steady state with respect to the level of node concentration? Any simulation study associated with power-law distributions inherently possesses a similar convergence problem [33]. Essentially, such simulations can take a very long time to reach steady state and can be very variable even at steady state. In CMM, it means that the population of a hub subarea decreases and that of a sparse subarea increases as simulation time progresses. Therefore, it is difficult to obtain steady state network performance in a reasonable amount of simulation time. Based on our analysis, the steady-state population of a dense subarea converges to  $k_i(1 - \xi)$ , where  $k_i$  is the

---

### Notations:

$s_i$ : a subarea in a network, where  $0 \leq i < s_t$  ( $s_t$  is the total number of subareas).

$k_i$ : the number of nodes in the subarea  $s_i$ .

$\varphi_i$ : the probability that a node selects  $s_i$  as a destination subarea.

#### (A) Growth (initial layout):

/\* when a new node joins in the network, \*/

**for** ( $i = 0; i < s_t; i ++$ ) {

/\* calculate the popularity of subarea  $s_i$  \*/

$k_i \leftarrow$  subarea population of  $s_i$ ;

$\varphi_i \leftarrow \frac{(k_i+1)^\alpha}{\sum_j (k_j+1)^\alpha}$ ;

}

choose a destination subarea using  $\varphi_j$ 's;

choose a random position within the chosen subarea;

/\* when the network reaches the pre-determined number of nodes, \*/

**for** (each hub area  $s_i$  such that  $k_i \gg \frac{n}{s_t}$ ) {

/\* calculate the steady-state population \*/

$k'_i \leftarrow$  subarea population of  $s_i$  at steady-state ( $k_i(1 - \xi)$ );

}

choose a destination subarea randomly for each of the excluded nodes;

choose a random position within the chosen subarea;

#### (B) Rewiring (mobility):

/\* when a node moves in the network, \*/

select a subarea  $s_i$  based on final probability of  $\varphi_j$ 's;

within the  $s_i$ , the destination is chosen randomly;

---

Fig. 2. The pseudo code of the CMM.

population of the subarea just after the growth step. The CMM algorithm identifies a few hub subareas just after the growth step, e.g.,  $s_i$ . And then, it reduces its populations from  $k_i$  to  $k_i(1 - \xi)$ . Each of the excluded nodes is assigned one of the remaining subareas randomly. The overall CMM algorithm is summarized in Fig. 2.

There are three additional issues to be noted. First, two different interpretations of the preferential attachment mechanism, attracted to a node or to a subarea, are in fact not very different in spatial graphs as explained in Section II.A. A subarea with a hub node is essentially a hub subarea because a large number of connectivity of a hub node directly translates to a large number of nodes in the proximity. Second, the size of a subarea is carefully chosen so that a node in a subarea directly connects to most of the other nodes in the same subarea but those in neighboring subareas may or may not connect depending on their locations in the corresponding subareas. This paper uses the transmit range of the radio device (i.e., 250m) as each side of a subarea. Third, two-step process in the CMM algorithm may not produce a scale-free network in its original meaning mainly due to the mobility step. However, our goal in this paper is to offer a mobility model that induces node clustering in a controlled manner rather than one that strictly possesses the scale-free property. In addition, the two-step process makes the analysis tractable and makes it feasible to use with network simulator such as ns-2 [34]. Since ns-2 does not support incremental network growth and usually assumes that the number of nodes is pre-determined.

### B. Analysis of CMM

Fig. 3 compares node distributions of CMM ( $\alpha = 1.2$  and  $\alpha = 1.4$ ) with RWP\_WRAP. In fact, RWP\_WRAP is

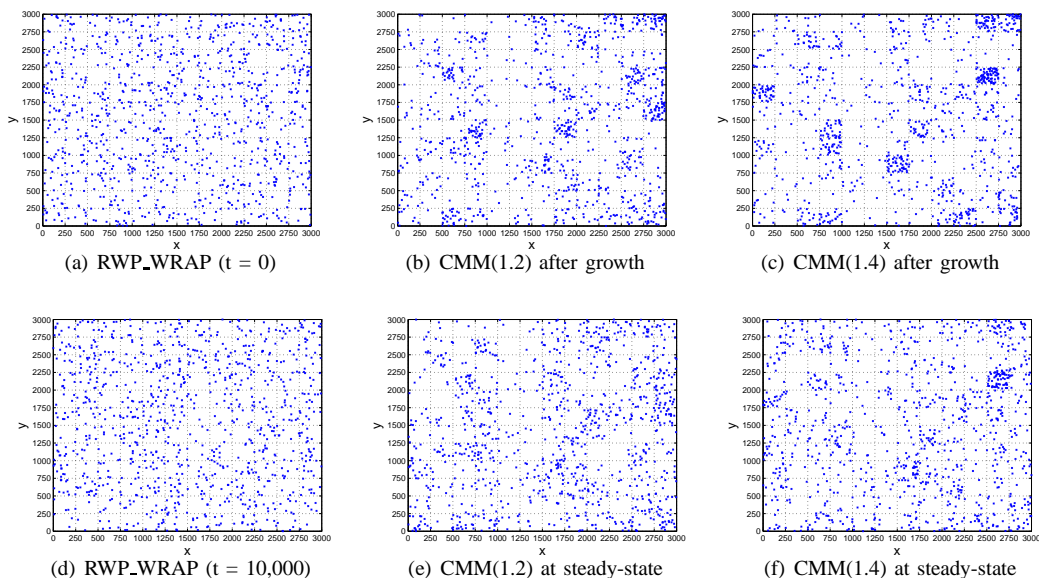


Fig. 3. Node distributions in RWP\_WRAP and CMM models ( $N = 1,000$ ,  $5 \leq v \leq 20.0$  (m/sec), and  $T_{pause} = 106$  (sec)).  $\alpha$  is set to be 1.2 (CMM(1.2)) for (b) and (e) and 1.4 (CMM(1.4)) for (c) and (f). Subfigures (a), (b), and (c) show the layouts before adjustment for steady-state. Subfigures (d), (e), and (f) can be considered initial layouts after the steady-state adjustment.

considered a special case of CMM when  $\alpha$  is zero. Total number of nodes is assumed to be 1000 in the network area of  $3000 \times 3000 m^2$  and node speed is chosen from [5, 20]. From Figs. 3(a) and (d), it would be safe to say that RWP\_WRAP provides random as well as consistent node distribution during simulation. In CMM(1.2), the level of node concentration is higher in Fig. 3(b) than in Fig. 3(e), which are before and after the adjustment for steady state layout. In Figs. 3(c) and (f), the same phenomenon is observed while nodes are more cluttered than the case with  $\alpha = 1.2$ .

Now, consider the rewiring step of CMM. It produces a combination of random and scale-free networks as mentioned earlier in the previous subsection. Mobility fraction,  $\xi$ , which was defined as the fraction of time a node moves during its lifetime, is used to elaborate more in this regard. Higher the node speed, lower the mobility fraction. And, smaller the pause time, lower the mobility fraction. Note that network size also affects the mobility fraction because a node moves for a longer duration of time to reach a destination in a larger network. For example, consider an example network where a node chooses its speed from [5, 20] m/sec and pauses for 60 seconds in  $3000 \times 3000 m^2$  network area. It is not difficult to show that average internodal distance is about 1148m (remember it is a wrap-around network) and that average move time is about 106 seconds. Since pause time is 60 seconds,  $\xi = \frac{106}{60+106} = 64\%$ . It can be interpreted that a node is randomly located in the network for 64% ( $\xi$ ) of the time but located in a scale-free fashion for the rest of the time (36% or  $1-\xi$ ). Here, we exclude an analysis of steady-state behavior due to space limitation.

#### IV. PERFORMANCE EVALUATION

This section presents several capacity measures that provide in-depth information about the network capability and make it possible to prepare provisions to optimize the network operation. Since our primary goal is to understand the maximum

achievable capacity rather than the mechanism to achieve it, we make several simplifying assumptions discussed in detail later in this section. Section IV-A defines three capacity measures and Section IV-B presents the comparison of SFWNs and WNs, driven by CMM and RWP\_WRAP mobility models, respectively, via simulation.

##### A. Capacity Measures

Before presenting the network scenario and evaluation results, we define three capacity measures for use in the simulation. They are *PHY (nearest one-hop) capacity*, *MAC (one-hop) capacity*, and *NET (multihop) capacity*.

1) *PHY (nearest one-hop) Capacity*: PHY capacity measures how much traffic the network can support without regard to the sender-receiver distance. According to Grossglauer and Tse [35], the network capacity is constrained by the mutual interference of concurrent transmission between nodes but can be maximized by allocating the channel resource to the node that can best exploit it, which encourages in communications between nearest neighbors. Multiple communications can happen simultaneously as long as their *signal-to-interference ratio* (SIR) is larger than a certain threshold, called *capture ratio* [36]. Since signal strength greatly depends on communication distance, a transmission between nearest neighbors can survive with a high probability even in the presence of interference in its proximity.

This paper shows two versions of PHY capacities: the number of successful concurrent transmissions using a fixed capture ratio (10 dB or 6 dB) and the sum of achievable throughput. For the latter, achievable throughput of each link is computed based on the Shannon's theorem. In other words, maximum achievable link capacity is calculated as  $W \log(1 + SIR)$ , where  $W$  is the link bandwidth.

2) *MAC (one-hop) Capacity*: While nearest-neighbor communication is attractive with respect to PHY capacity, network layer protocols developed for multihop networks usually favor

farthest-neighbor communications as long as they are along the direction of a final destination. In conventional carrier sense (CS) based MAC protocols, such as IEEE 802.11 DCF [37], the PHY capacity cannot be achievable due to carrier sensing. When a node observes a carrier signal above the *CS threshold*, it holds up pending transmission requests to avoid collisions. In this paper, MAC capacity measures the number of concurrent transmissions, each of which offers higher SIR than a fixed capture ratio, *e.g.*, 10dB, and communicates with the farthest neighbor within the transmit range of a sender. A complete coordination is assumed so that no *hidden* or *exposed terminal* [38] exists. *Transmit power control* (TPC) [39][40] may help enhance the MAC capacity by allowing a node to adjust and optimize its radio transmit power to reach the receiver node but not more than that. A key benefit of TPC schemes is energy conservation but it also reduces interference allowing more concurrent data transfers. We do not explore this issue in this paper and assumes that every node uses the same transmit power.

3) *NET (multihop) Capacity*: The ultimate goal of a wireless ad hoc network is to deliver packets to the desired destination. NET capacity measures the robustness of multihop connections between a pair of nodes in the network. For a node pair  $i$  and  $j$ , *connectivity* of the pair,  $\kappa_{i,j}$  is defined as the minimum number of nodes that need to be removed to disconnect the pair. It has been shown that  $\kappa_{i,j}$  is equal to the number of node-independent paths between the pair [41].  $\kappa_{i,j}$  is a direct measure of the resilience of the pair to node failure or node mobility. Also, it is considered a network-level forwarding capacity for the node pair because those multiple paths can simultaneously be utilized to deliver high volume of traffic as long as the source and the destination can sustain the traffic.

Generally, a network is said to have connectivity  $\kappa$  if removal of fewer than  $\kappa$  nodes will not increase the number of nodes of the connected network. It is also equivalent to the pairwise minimum of node-independent paths over all node pairs in the network [41]. Since computing such number for a given network is known to be NP-hard, this paper uses an approximation algorithm presented in [41]. According to it,  $\kappa_{i,j}$  can be obtained by finding the shortest path, finding the next shortest path using the unused nodes, and so on, until no further path exists for the node pair  $i$  and  $j$ . It is in fact a lower bound of  $\kappa_{i,j}$ . This paper uses this value and takes the minimum of  $\kappa_{i,j}$ 's for all possible pairs to obtain the NET capacity.

## B. Performance Analysis

As in Section III, we use 1000 mobile nodes located in a  $3000 \times 3000 m^2$  rectangular area. Each node follows CMM or RWP\_WRAP with a maximum node speed of  $20 m/s$  and a minimum node speed of  $5 m/s$ . The pause time ( $T_{pause}$ ) is set to 106 seconds to make the mobility factor 50%. The radio transmission range is assumed to be  $250 m$ .

Fig. 4 shows the node connectivity after the growth step and at steady-state. Nodes in hub subareas have been relocated to achieve the level of node concentration at steady-state. Figs. 4(a) and (c) correspond to the statistics just after the growth

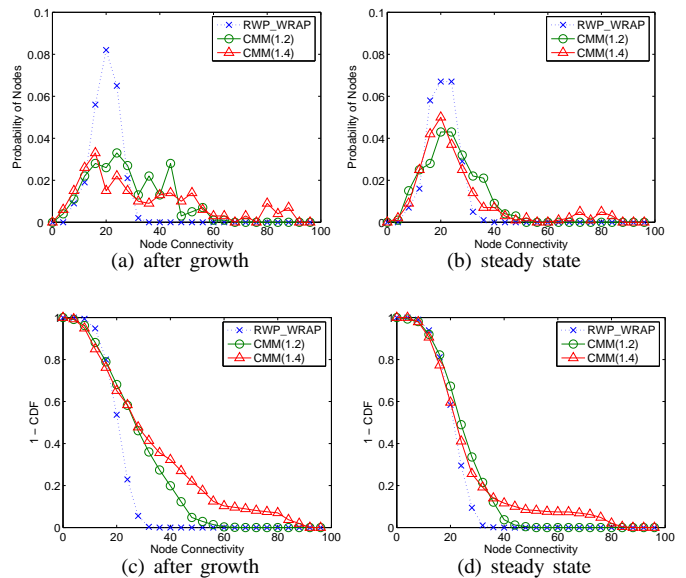


Fig. 4. Node connectivity in RWP\_WRAP and CMM models ( $N = 1,000$ ,  $5 \leq v \leq 20.0$  (m/sec), and  $T_{pause} = 106$  (sec)).

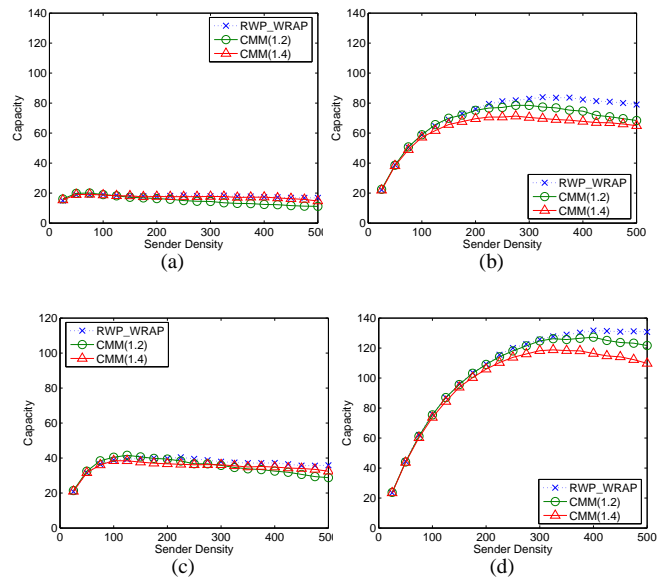


Fig. 5. PHY capacities in RWP\_WRAP and CMM models ( $N = 1,000$ ,  $5 \leq v \leq 20.0$  (m/sec),  $T_{pause} = 106$  (sec)). The path loss exponent is set to be 2 for (a) and (c) and 3 for (b) and (d). Also, the capture ratio is set to be 10 dB for (a) and (b) and 6 dB for (c) and (d).

step and Figs. 4(b) and (d) correspond to those at steady-state. Figs. 4(a) and (b) show the probability of nodes that has the corresponding connectivity and Figs. 4(c) and (d) show its cumulative statistics. For RWP\_WRAP, steady-state data was measured after executing the simulation for 10,000 seconds. As seen in the figure, RWP\_WRAP demonstrates very different connectivity distribution than CMM, which clearly shows a heavy-tail as in Figs. 4(c) and (d). This heavy-tail explains the existence of hub subareas. Also, as expected, the heavy-tail of CMM is larger just after the growth step (Fig. 4(c)) compared to that at steady state (Fig. 4(d)).

Fig. 5 compares average PHY capacity of CMM(1.2) and CMM(1.4) with RWP\_WRAP. For this experiment, we need to determine the *path loss exponent* which is a key parameter

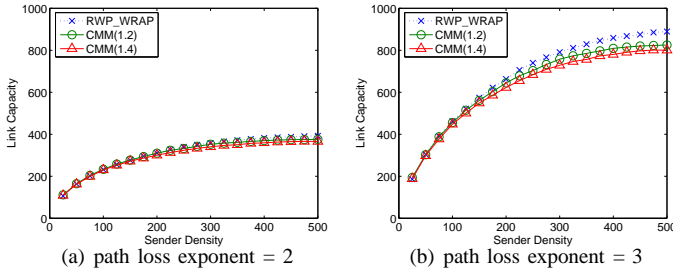


Fig. 6. PHY link capacities in RWP\_WRAP and CMM models ( $N = 1,000$ ,  $5 \leq v \leq 20.0$  (m/sec),  $T_{pause} = 106$  (sec), and capture ratio = 10 dB).

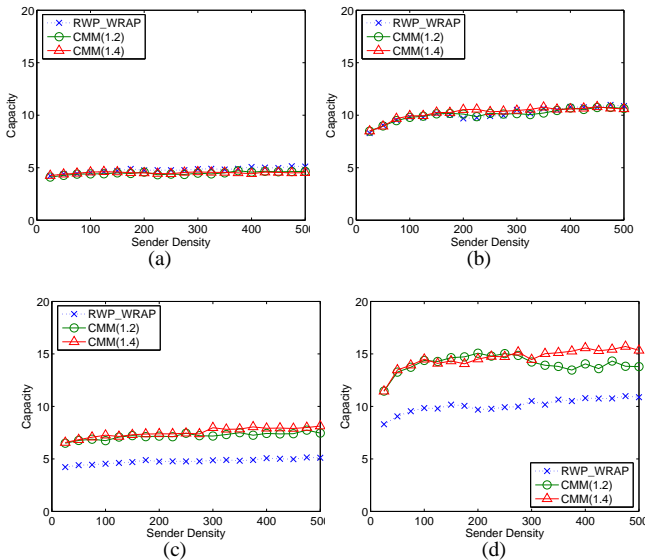


Fig. 7. MAC capacities in RWP\_WRAP and CMM models ( $N = 1,000$ ,  $5 \leq v \leq 20.0$  (m/sec),  $T_{pause} = 106$  (sec)). The path loss exponent is set to be 2 for (a) and (c) and 3 for (b) and (d). Also, the capture ratio is set to be 10 dB for (a) and (b) and 6 dB for (c) and (d).

in packet radio communication. Propagation in the mobile channel is described by means of three effects: attenuation due to distance between the sender and the receiver, shadowing due to the lack of visibility between the two nodes, and fading due to multipath propagation. The most popular two-ray ground propagation model is a simple propagation model that considers only the path loss due to communication distance. In other words, the mean received signal power follows an inverse distance power loss law, where an exponent assumes values between 2 and 4, and is typically 4 in land mobile radio environments. In the 915 MHz WaveLAN radio hardware, the transmit power is 24.5 dBm and the receive sensitivity is -72 dBm, which is translated to 250m or shorter distance between the sender and the receiver for successful communication.

As shown in the Fig. 5, CMM exhibits a comparable performance with RWP\_WRAP. With a larger path loss exponent, signal strength attenuates more rapidly and therefore, it opens a window for other pairs to communicate increasing the communication concurrency. Figs. 5(c) and (d) show a similar comparison with the capture ratio of 6 dB, which means the communication has a better chance to be successful even if its SIR is smaller. With a smaller capture ratio, the network can achieve a higher throughput but at the cost of increased cost for radio hardware. Capture ratio of 0 dB is the case of

TABLE I  
AVERAGE  $\kappa$ .

mobility	RWP_WRAP	CMM(1.2)	CMM(1.4)
$\kappa$	15.747626	12.799852	11.868478

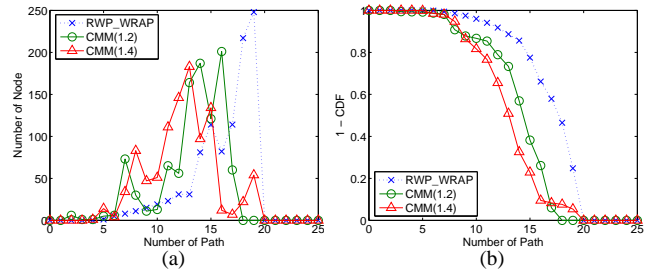


Fig. 8. NET capacities in RWP\_WRAP and CMM models ( $N = 1,000$ ,  $5 \leq v \leq 20.0$  (m/sec), and  $T_{pause} = 106$  (sec)).

perfect capture.

Fig. 6 shows another PHY capacity, where we do not incorporate the capture ratio. Instead, we assume that each radio device can communicate at any achievable data rate allowed by the radio environment in the proximity. For each pair of nodes, a receiver node calculates its SIR and thus the maximum data rate using the Shannon's theorem. Fig. 6 shows the aggregate throughput assuming that the link bandwidth is unity. As seen in the figure, CMM performs similarly as the RWP\_WRAP. Again, the path loss exponent significantly affects the performance as in Figs. 6(a) and (b).

Second, we present the results on MAC capacity in Fig. 7. As discussed earlier, each of the senders transmits to its farthest possible neighbor within its transmit range. Here, it is shown that RWP\_WRAP performs worse than CMM. As the sender density increases, the MAC capacity of RWP\_WRAP and CMM shows consistent performance. Path loss exponent plays a key role in determining the maximum performance as well. Comparing Figs. 7(a) and (b), and 7(c) and (d) shows that the network throughput is almost double in both of CMM and RWP\_WRAP.

Finally, results of NET capacity are presented in Table I and Fig. 8. Table I shows the average number of connectivity of a node pair. Also, Fig. 8(a) shows the number of node that has the corresponding number of node and Fig. 8(b) shows its cumulative statistics. As seen in the table and figure, RWP\_WRAP has more number of paths than CMM, due to uniform node distribution.

## V. CONCLUDING REMARKS

The main theme of this paper is to develop a new mobility model, called clustered mobility model (CMM), which allows non-homogeneous node distribution driven by two principles: network growth and preferential attachment. The level of non-homogeneity is controllable in CMM by changing the clustering exponent,  $\alpha$ , and is engineered not to vary during the simulation. For this, we represent the non-homogeneity with the distribution of subarea population and mobility fraction,  $\xi$ . Another important feature of CMM is that the mobility parameters such as node speed, positions and density reach the

steady state as quickly as possible so that one can reasonably believe the simulation results without worrying about the variability of the parameters or executing the simulation for an extended period of time.

To assess the strength and weakness of the scale-free phenomena, this paper defines network capacities at PHY, MAC and NET layers. Based on simulation-based performance analysis, we observed that SFWNs exhibit lower NET capacity but achieve higher MAC and as high PHY capacity as conventional wireless networks. This suggests us that a SFWN requires a unique network-layer solution. We believe that the proposed CMM can be usefully used to investigate the properties of the SFWNs that are likely to occur in a real deployment of wireless multihop and sensor networks.

## REFERENCES

- [1] S. H. Strogatz, "Exploring complex networks," *Nature*, vol. 410, pp. 268–276, 2001.
- [2] A. L. Barabasi and E. Bonabeau, *Scale-free networks*. Scientific American, 288 (50-59), 2003.
- [3] Erdős and Rényi, "On the evolution of random graphs," *Publ. Math. Inst. Hungar. Acad. Sci.*, vol. 5, pp. 17–61, 1960.
- [4] G. Németh and G. Vatty, "Giant Clusters in Random Ad Hoc Networks," in *e-print cond-mat/0211325*, 2003.
- [5] V. Kawadia and P. Kumar, "Power Control and Clustering in Ad Hoc Networks," in *Proc. IEEE INFOCOM*, 2003, pp. 459–469.
- [6] K. Wang and B. Li, "Group Mobility and Partition Prediction in Wireless Ad-Hoc Networks," in *Proc. IEEE ICC*, 2002, pp. 1017–1021.
- [7] S. Lee and A. Campbell, "HMP: Hotspot Mitigation Protocol for Mobile Ad Hoc Networks," in *Proc. 11th IEEE/IFIP Int'l Workshop on Quality of Service*, 2003, pp. 266–286.
- [8] D. B. Johnson and D. A. Maltz, "Dynamic Source Routing in Ad Hoc Wireless Networks," in *Mobile Computing*, Kluwer 1996, pp. 153–181.
- [9] W. Navidi and T. Camp, "Stationary Distributions for the Random Waypoint Mobility Model," *IEEE Trans. on Mobile Computing*, vol. 3, no. 1, pp. 99–108, 2004.
- [10] B. Christian, H. Hannes, and C. Xavier, "Stochastic Properties of the Random Waypoint Mobility Model," *Wireless Networks*, vol. 10, no. 5, pp. 555–567, 2004.
- [11] J. Yoon, M. Liu, and B. Noble, "Random Waypoint Considered Harmful," in *Proc. IEEE INFOCOM*, 2003, pp. 1312–1321.
- [12] J. Amit, B. Elizabeth, A. Kevin, and S. Subhash, "Towards Realistic Mobility Models for Mobile Ad Hoc Networks," in *Proc. IEEE MOBI-COM*, 2003, pp. 217–229.
- [13] L. Guolong, N. Guevara, and R. Rajmohan, "Mobility Models for Ad Hoc Network Simulation," in *Proc. IEEE INFOCOM*, 2004, pp. 454–463.
- [14] C. Bettstetter, G. Resta, and P. Santi, "The Node Distribution of the Random Waypoint Mobility Model for Wireless Ad Hoc Networks," *IEEE Trans. on Mobile Computing*, vol. 2, no. 3, pp. 257–269, 2003.
- [15] B. M. Douglas, R. Giovanni, and S. Paolo, "A Statistical Analysis of the Long-run Node Spatial Distribution in Mobile Ad Hoc Networks," *Wireless Networks*, vol. 10, no. 5, pp. 543–554, 2004.
- [16] F. Bai, N. Sadagopan, and A. Helmy, "The IMPORTANT Framework for Analyzing the Impact of Mobility on Performance of Routing for Ad Hoc Networks," *Ad Hoc Network Journal*, vol. 4, pp. 383–403, 2003.
- [17] E. M. Royer, P. M. Melliar-Smith, and L. E. Moser, "An Analysis of the Optimum Node Density for Ad Hoc Mobile Networks," in *Proc. IEEE ICC*, 2001, pp. 857–861.
- [18] D. J. Watts and S. H. Strogatz, "Collective dynamics of 'small-world' networks," *Nature*, no. 393, pp. 440–442, 1998.
- [19] A. L. Barabasi and R. Albert, "Emergence of scaling in random networks," *Science*, vol. 286, pp. 509–512, 1999.
- [20] W. E. Leland, M. S. Taqqu, W. Willinger, and D. V. Wilson, "On the Self-Similar Nature of Ethernet Traffic," *IEEE/ACM Transactions on Networking*, pp. 1–15, 1994.
- [21] M. Harchol-Balter and A. B. Downey, "Exploiting Process Lifetime Distributions for Dynamic Load Balancing," in *ACM SIGMETRICS*, 1996, pp. 13–24.
- [22] M. F. Arlitt and C. L. Williamson, "Web server workload characterization: The search for invariants," in *ACM SIGMETRICS*, 1996, pp. 126–137.
- [23] R. Albert and A. L. Barabasi, "Topology of Evolving Networks: Local Events and Universality," *Physical Review Letters*, vol. 85, no. 24, pp. 5234–5237, 2000.
- [24] Q. Chen, H. Chang, R. Govindan, S. Jamin, S. Shenker, and W. Willinger, "The Origin of Power Laws in Internet Topologies Revisited," in *IEEE Infocom*, 2002.
- [25] D. ben Avraham, A. F. Rozenfeld, R. Cohen, and S. Havlin, "Geographical Embedding of Scale-Free Networks," in *e-print cond-mat/0301504*, Jan 2003.
- [26] C. Herrmann, M. Barthélemy, and P. Provero, "Connectivity Distribution of Spatial Networks," in *e-print cond-mat/0302544*, Feb 2003.
- [27] T. Camp, J. Boleng, and V. Davies, "A Survey of Mobility Models for Ad Hoc Network Research," *Wireless Communications Mobile Computing (WCMC): Special Issues on Mobile Ad Hoc Networking: Research, Trends, and Applications*, vol. 2, no. 5, pp. 483–502, 2002.
- [28] A. Bar-Noy, I. Kessler, and M. Sidi, "Mobile Users: To Update or Not To Update?" *Wireless Networks*, vol. 1, no. 2, pp. 175–185, 1995.
- [29] G. Wan and E. Lin, "Cost Reduction in Location Management Using Semi-realtime Movement Information," *Wireless Networks*, vol. 5, pp. 245–256, 1999.
- [30] Z. Biao, X. Kaixin, and G. Mario, "Group and Swarm Mobility Models for Ad Hoc Network Scenarios Using Virtual Tracks," in *Proc. IEEE Milcom*.
- [31] E. R. Sullivan, *One Nation: America Remembers September 11, 2001*. Time Warner Trade Publishing, 2001.
- [32] G. Ingmar, K. Wolfram, S. Rudolf, and G. Martin, "Continuum Percolation of Wireless Ad Hoc Communication Networks," *Statistical Mechanics; Disordered Systems and Neural Networks, Journal-ref: Physica A*, vol. 325, pp. 577–600, 2003.
- [33] M. E. Crovella and L. Lipsky, "Long-Lasting Transient Conditions in Simulations with Heavy-tailed Workloads," in *Winter Simulation Conference*, 1997.
- [34] *VINT Project, The UCB/LBNL/VINT network simulator-ns (Version 2)*, <http://www.isi.edu/nsnam/ns>.
- [35] M. Grossglauser and D. Tse, "Mobility Increases the Capacity of Ad-hoc Wireless Networks," in *IEEE INFOCOM*, 2001.
- [36] M. Zorzi and R. Rao, "Capture and retransmission control in mobile radio," *IEEE Journal on Selected Areas in Communications*, vol. 12, no. 8, pp. 1289–1298, 1994.
- [37] "IEEE Std 802.11-1999, Local and Metropolitan Area Network, Specific Requirements, Part 11: Wireless LAN Medium Access Control (MAC) and Physical Layer (PHY) Specifications," in <http://standards.ieee.org/getieee802/download/802-11-1999.pdf>, 1999.
- [38] W. Stallings, *IEEE 802.11 Wireless LAN Standard*. Prentice Hall, Inc., 2002, Chapter 14, Wireless Communications and Networks.
- [39] S. Narayanaswamy, V. Kawadia, R. S. Sreenivas, and P. R. Kumar, "Power Control in Ad-Hoc Networks: Theory, Architecture, Algorithm and Implementation of the COMPOW Protocol," in *European Wireless Conference*, 2002, pp. 156–162.
- [40] C. Yu, K. G. Shin, and B. Lee, "Power-Stepped Protocol: Enhancing Spatial Utilization in a Clustered Mobile Ad Hoc Network," *IEEE Journal on Selected Areas in Communications*, vol. 22, no. 7, pp. 1322–1334, Sep. 2004.
- [41] D. R. White and M. E. J. Newman, "Fast approximation algorithms for finding node-independent paths in networks," in *Working Papers 01-07-035, Santa Fe Institute*, 2001.